Cell Calcium 50 (2011) 433–443

Contents lists available at ScienceDirect

Cell Calcium

journal homepage: www.elsevier.com/locate/ceca

Adenylyl cyclase/cAMP-PKA-mediated phosphorylation of basal L-type Ca^{2+} channels in mouse embryonic ventricular myocytes

Xisheng Yan[a], Shijun Gao[a], Ming Tang[a], Jiaoya Xi[a], Linlin Gao[a], Minjie Zhu[a], Hongyan Luo[a], Xinwu Hu[a], Yunjie Zheng[a], Jürgen Hescheler[b], Huamin Liang[a,*]

[a] Department of Physiology, Tongji Medical College, Huazhong University of Science and Technology, Hangkong Road 13, 430030 Wuhan, Hubei, China
[b] Institute of Physiology, University of Cologne, Cologne, Germany

ARTICLE INFO

Article history:
Received 10 February 2011
Received in revised form 16 June 2011
Accepted 12 July 2011
Available online 7 August 2011

Keywords:
Cardiac electrophysiology
L-type Ca^{2+} channels
Protein kinase A phosphorylation
Protein phosphatase
Cardiogenesis

ABSTRACT

In fetal mammalian heart, constitutive adenylyl cyclase/cyclic AMP-dependent protein kinase A (cAMP-PKA)-mediated phosphorylation, independent of β-adrenergic receptor stimulation, could under such circumstances play an important role in sustaining the L-type calcium channel current ($I_{Ca,L}$) and regulating other PKA dependent phosphorylation targets. In this study, we investigated the regulation of L-type Ca^{2+} channel (LTCC) in murine embryonic ventricles. The data indicated a higher phosphorylation state of LTCC at early developmental stage (EDS, E9.5–E11.5) than late developmental stage (LDS, E16.5–E18.5). An intrinsic adenylyl cyclase (AC) activity, PKA activity and basal cAMP concentration were obviously higher at EDS than LDS. The cAMP increase in the presence of isobutylmethylxanthine (IBMX, nonselective phosphodiesterase inhibitor) was further augmented at LDS but not at EDS by chelation of intracellular Ca^{2+} with 1,2-bis(2-aminophenoxy)ethane-N,N,N′,N′-tetraacetic acid (BAPTA)-acetoxymethyl ester (BAPTA-AM). Furthermore, $I_{Ca,L}$ increased with time after patch rupture in LDS cardiomyocytes dialyzed with pipette solution containing BAPTA whereas not at EDS. Thus we conclude that the high basal level of LTCC phosphorylation is due to the high intrinsic PKA activity and the high intrinsic AC activity at EDS. The latter is possibly owing to the little or no effect of Ca^{2+} influx via LTCCs on AC activity, leading to the inability to inhibit AC.

1. Introduction

Calcium influx through voltage-gated L-type calcium channels (LTCCs) is responsible for initiating excitation–contraction coupling in the heart [1–5]. L-type Ca^{2+} current ($I_{Ca,L}$) is dynamically regulated by the second messenger-activated protein kinases, phosphatases, and G proteins [1,2,6,7]. Increased activity of LTCCs owing to activation of β-adrenergic receptors and phosphorylation by cAMP-dependent protein kinase A (cAMP-PKA) contributes to the increase in beating rate and contractile force upon activation of the sympathetic nervous system [1,2,6,8]. Because of the relative paucity of sarcoplasmic reticulum in embryonic cardiocytes, $I_{Ca,L}$ contributes proportionally more to the excitation–contraction (EC coupling) in the embryo than in the adult [9,10]. Three different LTCCs, $Ca_v1.1$, $Ca_v1.2$, and $Ca_v1.3$, have been identified in embryonic hearts [11–13]. Among these channels, $Ca_v1.2$ is the predominantly expressed isoform in cardiomyocytes [12]. $Ca_v1.2$ consists of a central α_1-subunit (designated $\alpha_1 1.2$), which forms the ion-conducting pore, and the auxiliary subunits α_2, -δ, -β, and -γ. Only $\alpha_1 1.2$, and none of the auxiliary subunits is required for the PKA-mediated increase in channel activity [14]. $\alpha_1 1.2$ embodies six potential phosphorylation sites by PKA [15]. However, serine 1928 seems to be the only site that could be phosphorylated by PKA [16–18].

Most previous studies have found that $I_{Ca,L}$ densities increase in the whole-cell-recording configuration during embryonic heart development, little attention has been paid to single-channel properties of LTCCs. LTCCs are responsive to isoproterenol (ISO) and 8-bromo-cAMP (8-Br-cAMP) at late developmental stage (LDS) but not at early developmental stage (EDS) [19–21]. Thus, it is hypothesized that a phosphorylation-related mechanism is responsible for the high activity of channels in EDS cardiomyocytes. Despite recent advances in the understanding of the cAMP-PKA-mediated phosphorylation of the LTCCs during embryonic development [21], it remains unclear as to whether cAMP-PKA also sustains the basal $I_{Ca,L}$ observed during cardiomyocyte development in the absence of β-adrenergic receptor stimulation. The regulation of cAMP pulsatile concentration is mediated by two sets of enzymes, adenylate cyclases (AC) and phosphodiesterases (PDE) [22–24]. Although a reduction in PDE activity could, in part, account for high levels of cAMP at EDS, recent evidence suggests that basal PDE activity is not reduced in EDS

* Corresponding author. Tel.: +86 27 83691903; fax: +86 27 83691903.
E-mail address: lianghuamin@hotmail.com (H. Liang).

0143-4160/$ – see front matter © 2011 Elsevier Ltd. All rights reserved.
doi:10.1016/j.ceca.2011.07.004

cardiomyocytes, but rather, appears to be elevated [21]. The previous study has proved indirectly that EDS cells are characterized by high intrinsic AC activity in murine embryonic stem cell-derived cardiomyocytes [21,25]. In cardiac myocytes where AC5 and AC6 are the most abundant isoforms, inhibition of AC activity results primarily from the activation of LTCCs [26,27]. In addition, protein phosphatases are colocalized with LTCCs and can also tonically regulate the phosphorylation status of the channel to modulate $I_{Ca,L}$ [28–30]. Therefore, the constitutive mechanisms that determine the basal levels of channel phosphorylation are important determinants of $I_{Ca,L}$ regulation in embryonic cardiocytes.

Thus we aimed to investigate AC/cAMP-PKA-mediated phosphorylation of basal LTCCs in murine embryonic ventricles, and found that the single-channel activity of LTCCs was substantially higher in EDS than LDS cardiomyocytes. The profile of the enhanced activity of channels at EDS closely resembled the effects of a cAMP-dependent stimulation. Besides, our results echoed the previous research which suggested that LTCCs were responsive to ISO and 8-Br-cAMP at LDS but not at EDS [19–21]. The intrinsic PKA activity and basal cAMP concentration were obviously higher in EDS than LDS cardiomyocytes. Moreover, EDS cells were characterized by high intrinsic AC activity. The high intrinsic AC activity was possibly due to the little or no effect of Ca^{2+} influx via LTCCs on AC activity, leading to the inability to inhibit AC at EDS.

2. Materials and methods

2.1. Preparation of embryonic ventricular myocytes

Embryos were removed from pregnant female Kunming mice. E9.5–E11.5 and E16.5–E18.5 embryos were taken as EDS and LDS, respectively. Briefly, after embryos were harvested, hearts were dissected and atria were separated from ventricles. Single ventricular cardiomyocytes were obtained using enzymatic dissociation procedures as described previously [31,32], then were plated on sterile gelatin-coated glass cover slips, cultured in Dulbecco's Modified Eagle's Medium (DMEM, Gibco) containing 20% fetal bovine serum and kept in the incubator for 24–48 h for electrophysiological experiments.

2.2. Electrophysiology

Standard voltage clamp recordings were performed using the classic patch-clamp technique. Current was recorded using an EPC-10 amplifier/interface (HEKA Electronics, Lambrecht/Pfalz, Germany). Glass coverslips with cardiomyocytes were transferred to the temperature-controlled (37 °C) recording chamber and placed upon the stage of an inverted microscope (IX-70, Olympus Optical Co., Japan). The cells were constantly superfused using a gravitational perfusion system at a perfusion rate of about 2 ml/min with experimental external solutions (in mM): 120 NaCl, 5 KCl, 2 $CaCl_2$, 20 tetraethylammonium-Cl, 1 $MgCl_2$ and 10 HEPES (pH adjusted to 7.4 with TEA-OH). For whole-cell recordings, pipettes resistances were in the range of 2–4 MΩ when filled with intracellular solution containing (in mM): 120 CsCl, 3 $MgCl_2$, 5 MgATP, 10 EGTA and 5 HEPES (pH adjusted to 7.4 with CsOH). To avoid contamination by Na^+ channels, TTX (Tetrodotoxin citrate, 15 μmol/L) was administrated. In order to explore whether $I_{Ca,L}$ was augmented by 1,2-bis(2-aminophenoxy)ethane-N,N,N′,N′-tetraacetic acid (BAPTA) in EDS and LDS cardiomyocytes, the pipette solution was modified [33,34] as following (in mM): 50 mM CsCl, 51 mM cesium aspartate, 2 mM $MgCl_2$, 4 mM MgATP, 10 mM HEPES and 40 mM BAPTA (pH adjusted to 7.4 with CsOH). Whole-cell currents were recorded using two-pulse protocols from a holding potential of −80 mV to test potentials, following a 50 ms prepulse to −40 mV, which was useful to inactivate T-type Ca^{2+} current ($I_{Ca,T}$) [35,36]. The first was a standard *I–V* protocol for $I_{Ca,L}$. $I_{Ca,L}$ was elicited by 300 ms pulses to different test potentials (−50 to +50 mV), and the second was the single pulse to 0 mV with a duration of 300 ms. Single calcium channels were recorded in cell-attached configuration of the patch-clamp technique (depolarizing test pulses of 150 ms duration at 1.67 Hz, holding potential −80 mV, test potential +20 mV). The shanks of pipettes with resistance of 7–10 MΩ were coated with Sylgard, and the tips were heat polished. The pipette (extracellular) solution contained (in mM): 110 $BaCl_2$, 10 HEPES, 0.03 TTX (pH adjusted to 7.4 with TEA-OH). The bath (intracellular) solution contained (in mM) 25 KCl, 120 K-glutamate, 2 $MgCl_2$, 10 HEPES, 2 EGTA, 10 dextrose, 1 $CaCl_2$, 1 Na_2-ATP (pH adjusted to 7.4 with KOH). The calculated resting free [Ca^{2+}] was ∼50 nM for the solution with a low Ca^{2+} concentration [37]. This high-K^+ bath solution made the cell membrane potential close to zero, thus allowing accurate determination of the trans-patch potential. Capacitance and series resistances were adjusted to obtain minimal contribution of the capacitive transients. A 60–80% compensation of the series resistance was usually achieved without ringing. Currents were filtered at 2 kHz, digitized at 10 kHz and stored on a computer hard disk for analysis.

2.3. Western blot experiments

The CNC1 antibody used in these studies was an affinity purified rabbit polyclonal antibody, raised against a peptide covering residues 821–835 of $\alpha_1$1.2 (America Basic Gene Associate Bioscience, Inc). Anti-CH3P (Badrilla Ltd), a phosphospecific antibody, was generated against a phosphopeptide (residues 1923–1932) that encompasses the PKA consensus site at serine 1928 as described [18]. Proteins were separated on 7.5% SDS-polyacrylamide gels, blotted, and probed with antibodies by using a chemiluminescence detection system. To quantitatively evaluate serine 1928 phosphorylation, blots were first probed with Anti-CH3P antibody and subsequently with Anti-CNC1 antibody to correct for variability in the amount of total Ca_v1.2.

2.4. Measurement of cytosolic cAMP concentration

The cAMP concentrations of myocytes were measured using the method described by Narayan et al. [38] with a slight modification. The cells were incubated with one of the test compounds in Tyrode's solution for 10 min then pelleted by centrifugation (1 min, 1000 × *g*) and the supernatant was discarded. Myocytes were lysed in 500 μl of HCl (0.1 N, 10 min) and vortexed. The suspension was centrifuged (4 min, 3000 × *g*), and the supernatant was assayed for cAMP with ELISA kit (R&D Systems, MN). The pellet was solubilized with 1 N NaOH, and protein was assayed by the Lowry method. Intracellular cAMP was expressed as picomoles per milligram of protein.

2.5. Adenylyl cyclase assay

Adenylyl cyclase activity was measured as previously described [39]. A final [Ca^{2+}] of 0.2 or 1 μM at pH 7.4 and 30 °C was achieved by adding to the assay buffer 0.7336 or 0.9332 mM $CaCl_2$, respectively [37]. At the end of the incubation the medium was extracted to determine the cAMP as described above.

2.6. Data analysis

Whole-cell recordings were analyzed using PulseFit (V8.74, HEKA). Single-channel recordings were analyzed using TAC+TACFit (X4.0.9, Bruxton, Seattle, Washington, USA). Mostly, experiments

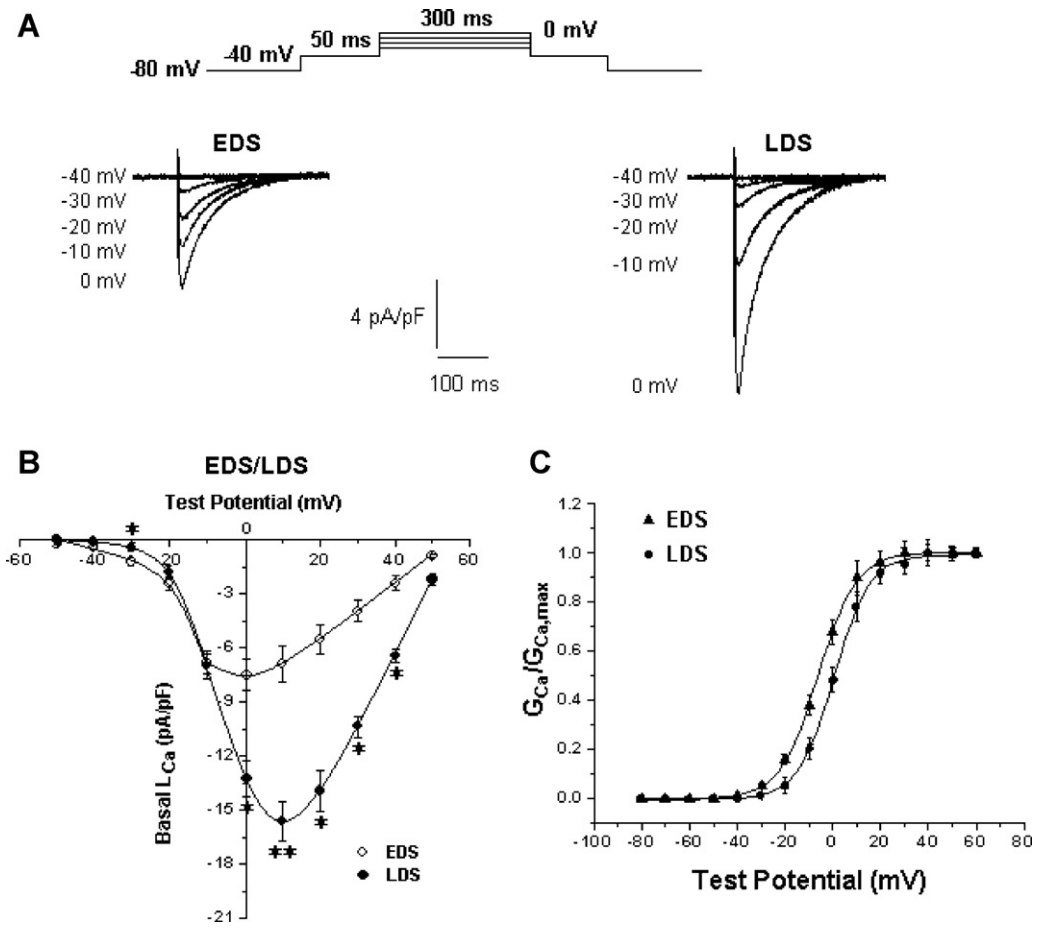

Fig. 1. Basic characterization of the L-type Ca^{2+} current ($I_{Ca,L}$) in embryonic ventricular cardiomyocytes. The current–voltage (*I–V*) relationship of $I_{Ca,L}$ was determined by applying test pulses (T, 300 ms) from −40 mV to 0 mV in 10 mV increments at a frequency of 0.2 Hz. Pre-pulses from a HP of −80 mV to −40 mV (P, duration: 50 ms) together with Tetrodotoxin (TTX, 15 μM) were applied to inactivate Na^+ currents (I_{Na}). According to the previous studies, the prestep to −40 mV is useful to inactivate also T-type Ca^{2+} current ($I_{Ca,T}$) (A *upper panel*). (A) Representative *I–V* traces recorded from early (EDS, *left panel*) and late (LDS, *right panel*) development stage cardiomyocyte. (B) Averaged *I–V* curves of peak $I_{Ca,L}$ in EDS ($n = 14$ cells from 4 hearts) and LDS cardiomyocytes ($n = 14$ cells from 5 hearts). (C) Voltage dependence of $I_{Ca,L}$ activation EDS and LDS cardiomyocytes were fit with Boltzmann Equation $G/G_{max} = 1/[1 + \exp(V_{0.5} - V)/k]$. $V_{0.5}$ at EDS (−6.58 ± 0.97 mV, $n = 12$ cells from 4 hearts) was more negative ($P < 0.01$) than in LDS (1.22 ± 1.04 mV, $n = 12$ cells from 4 hearts) cardiomyocytes. Slope factor of the activation curve (k) was not significantly different in the two groups (EDS versus LDS: 5.81 ± 0.07 versus 6.08 ± 0.18). Asterisks indicate statistically significant differences.

with one single channel (i.e., no stacked openings above unitary amplitude level) were analyzed in this study. Capacitance transients and leakage currents were nullified by off-line subtracting fits of average blunt traces. Openings and closures were identified by the half-height criterion. The fraction of active sweeps within a channel-containing patch (availability), the open probability within active sweeps (open probability), and the peak value of single-channel ensemble average currents (I_{peak}) were determined as described [40]. In case of double- or triple-channel patches, these parameters were corrected by the number of channels [41]. Time constants of open and closed-time histograms were estimated by the maximum-likelihood method [42]. The data acquired from western blot technique was quantified by determining the ratio of the Anti-CH3P antibody to the Anti-CNC1 signal for each sample by blot densitometry using Quantity One software (Bio-Rad). Data were presented as mean ± SEM. The statistical significance of effects was evaluated by Student's *t* test or ANOVA where appropriate. A value of $P < 0.05$ was considered statistically significant.

3. Results

3.1. Characteristics of the $I_{Ca,L}$ during development

As the basic characteristics of $I_{Ca,L}$, $I_{Ca,L}$ densities, *I–V* curves and voltage-dependence activation curves in EDS and LDS cardiomyocytes were determined (Fig. 1). The average cell capacitance was significantly smaller in cardiomyocytes derived from EDS than LDS ($P < 0.05$) (Table 1). As compared to LDS, at EDS a depolarization to −30 mV elicited a larger $I_{Ca,L}$ ($P < 0.05$) while the depolarizing pulse to 0 mV induced a smaller $I_{Ca,L}$ ($P < 0.01$) (Table 1). The current–voltage relationships (*I–V* curves) (Fig. 1B) and the activation curves (Fig. 1C) of $I_{Ca,L}$ obtained in EDS and LDS cardiomyocytes demonstrated more details of the developmental changes in characteristics of $I_{Ca,L}$. Both the threshold membrane potential for activation of $I_{Ca,L}$ and the potential of half-maximal activation ($V_{0.5}$) at EDS were more negative than that at LDS ($P < 0.05$) (Table 1).

3.2. Effects of ISO and 8-Br-cAMP on whole cell Ca^{2+} current

As seen in Fig. 2A, 1 μM ISO had only minor effects (+13.6 ± 2.9%) on $I_{Ca,L}$ amplitude at EDS ($n = 12$, P = NS), whereas it strongly stimulated $I_{Ca,L}$ at LDS (+76.4 ± 4.2%, $n = 12$, $P < 0.05$). 1 μM ISO also led to a shift of the voltage dependence of $I_{Ca,L}$ activation to more negative potentials at LDS (Fig. 2C, right panel), but had no significant effect at EDS (Fig. 2C, left panel). After ISO treatment, there were no significant differences in $V_{0.5}$ between these two groups (Fig. 2C). Noteworthily, the voltage dependence of $I_{Ca,L}$ activation was already set to the left at EDS under our basal conditions, and after ISO exposure, there was no further shift. These results sug-

Table 1
Basic characterization of the L-type Ca^{2+} currents in EDS and LDS cardiomyocytes.

Parameter	EDS	*n*	LDS	*n*
Average cell capacitance (pF)	38.5 ± 7.4	12	57.7 ± 10.2*	14
Threshold membrane potential for activation (mV)	−37.8 ± 3.46	10	−32.2 ± 2.15*	10
Potential of half-maximal activation (mV)	−6.58 ± 0.97	6	1.22 ± 1.04*	8
$I_{Ca,L}$ densities at test potential (−30 mV, pA/pF)	−1.2 ± 0.3	8	−0.4 ± 0.2*	10
$I_{Ca,L}$ densities at test potential (0 mV, pA/pF)	−7.5 ± 1.2	8	−13.2 ± 2.4**	10

EDS cardiomyocytes were from 4 different embryonic hearts, and LDS cardiomyocytes were from 5 different embryonic hearts. Values are expressed as mean ± SEM.
* $P < 0.05$ versus EDS group.
** $P < 0.01$ versus EDS group.

gest that there was an equivalent level of LTCC phosphorylation after ISO in all myocytes.

Likewise the LTCC activity in LDS but not EDS ventricular myocytes was sensitive to intracellular application of 8-Br-cAMP (Fig. 3A), a membrane permeable cAMP analogue that has previously been shown to enhance LTCC activity in the adult myocytes [43]. 8-Br-cAMP caused a leftward shift of voltage-dependent activation curves at LDS but no significant shift at EDS (Fig. 3C). Thus we hypothesize that the lack of ISO and 8-Br-cAMP effects on $I_{Ca,L}$ at EDS might result from the high level of basal LTCC phosphorylation.

3.3. Effects of PKI and okadaic acid on Ca^{2+} current

To investigate whether endogenous PKA played a role in sustaining basal $I_{Ca,L}$, myocytes were exposed to 15 μmol/L PKI, a membrane-permeable, specific peptide inhibitor of the PKA cat-

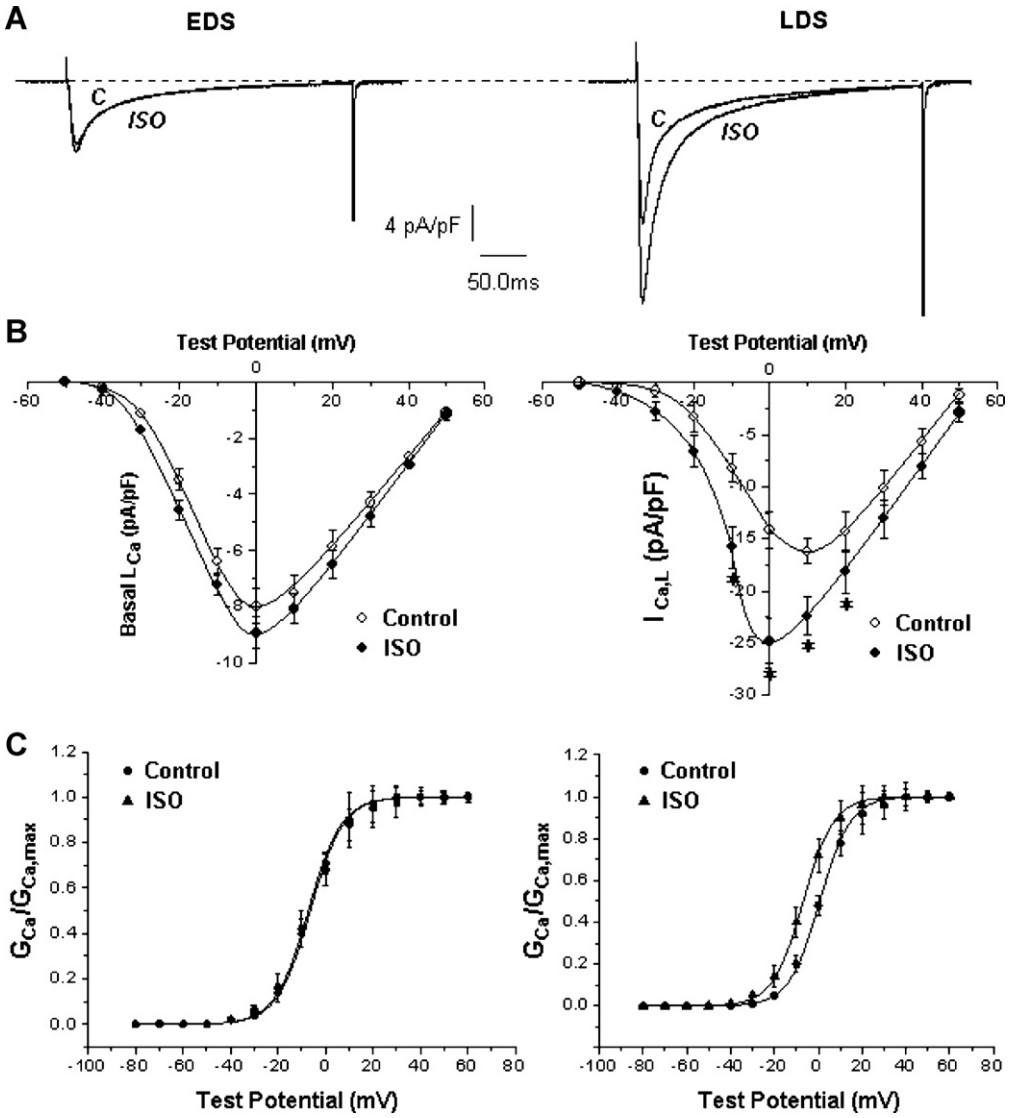

Fig. 2. Effects of 1 μmol/L ISO on $I_{Ca,L}$ in EDS ($n = 12$ cells from 4 hearts) and LDS ($n = 12$ cells from 5 hearts) cardiomyocytes. (A) Representative recordings of $I_{Ca,L}$ (test potential +0 mV) under control conditions and after application of ISO. (B) ISO increased $I_{Ca,L}$ at LDS but had little effect at EDS ($I_{Ca,L,ISO}/I_{Ca,L,C}$ at EDS versus LDS: 1.04 versus 1.51). (C) ISO led to a leftward shift of the voltage dependence of $I_{Ca,L}$ activation in LDS (change of $V_{0.5}$ (d_∞): −8.5 mV; $P < 0.05$) cardiomyocytes but no significant shift in EDS (change of $V_{0.5}$ (d_∞): −1.2 mV; P = NS) cardiomyocytes. After exposure to ISO, $V_{0.5}$ (d_∞) was not significantly different in the two groups (EDS versus LDS: 2.3 ± 0.3 versus 2.9 ± 0.5 mV) (P = NS). *Significant increase in $I_{Ca,L}$ at these voltages ($P < 0.05$).

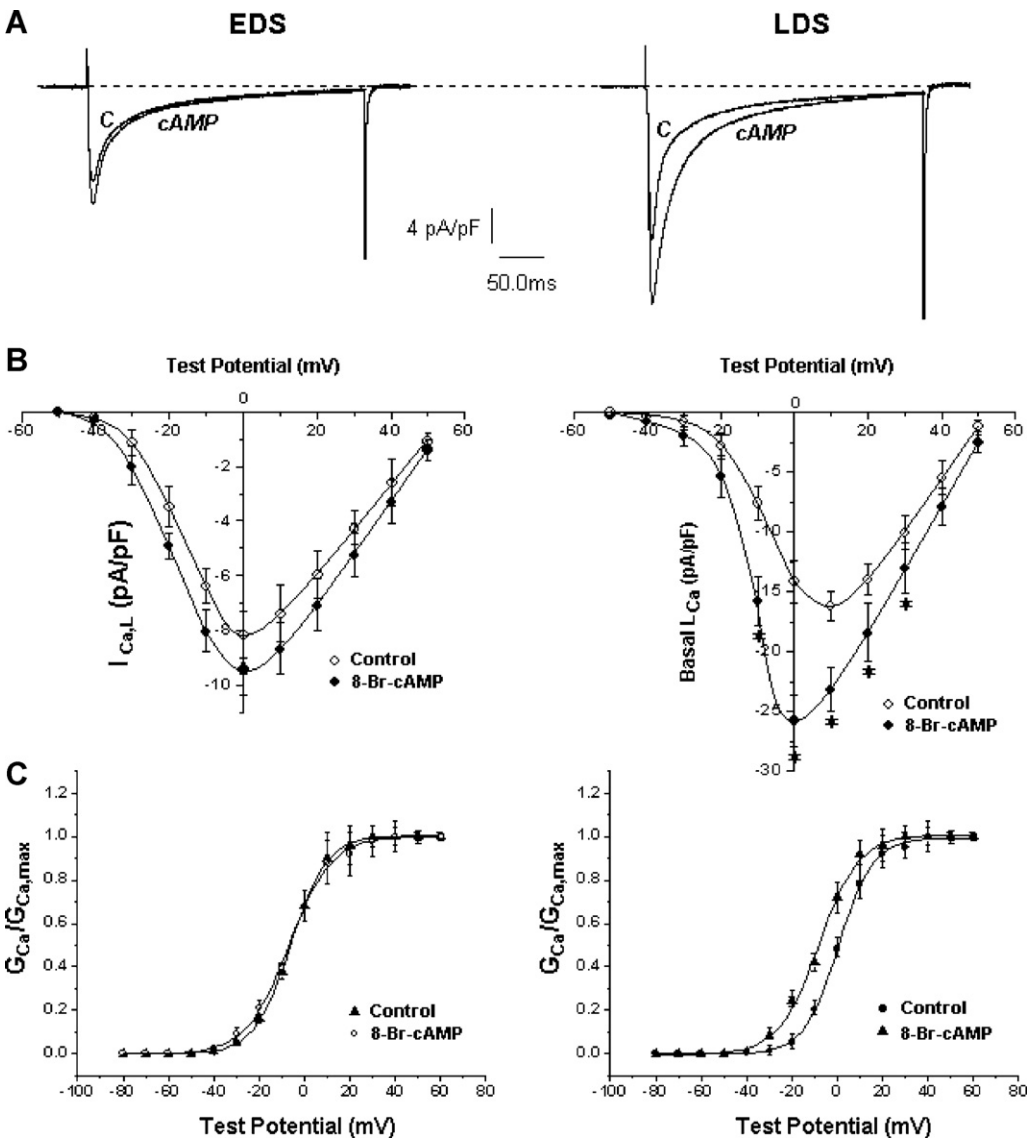

Fig. 3. Effects of 1 mmol/L 8-Br-cAMP on $I_{Ca,L}$ in EDS ($n = 10$ cells from 3 hearts) and LDS ($n = 13$ cells from 5 hearts) cardiomyocytes. (A) Representative recordings of $I_{Ca,L}$ (test potential +0 mV) under control conditions and after application of 8-Br-cAMP. (B) 8-Br-cAMP increased $I_{Ca,L}$ significantly at LDS but had little effect at EDS ($I_{Ca,L,cAMP}/I_{Ca,L,C}$ at EDS versus LDS: 1.06 versus 1.54). (C) 8-Br-cAMP caused a leftward shift of the voltage dependence of $I_{Ca,L}$ activation in LDS (change of $V_{0.5}$ (d_∞): −8.9 mV; $P < 0.05$) cardiomyocytes but no significant shift in EDS (change of $V_{0.5}$ (d_∞): −1.4 mV; P = NS) cardiomyocytes. After exposure to 8-Br-cAMP, $V_{0.5}$ (d_∞) was not significantly different in the two groups (EDS versus LDS: 2.1 ± 0.4 versus 2.5 ± 0.3 mV). *Significant increase in $I_{Ca,L}$ at these voltages ($P < 0.05$).

alytic subunit. PKI reversibly suppressed $I_{Ca,L}$, and the effects on peak $I_{Ca,L}$ was more significant at EDS than LDS (Fig. 4). In addition, H-89 (6 μmol/L), another PKA inhibitor, inclusion in the pipette solution resulted in an enhanced rundown of basal $I_{Ca,L}$ and displayed the a stronger inhibitory effect on peak $I_{Ca,L}$ at EDS (data not shown). Therefore, our results suggested a higher intrinsic PKA activity at EDS than LDS. Unexpectedly, the protein phosphatases 1/2A (PP1/PP2A) inhibitor okadaic acid (OA) (10 μmol/L) increased $I_{Ca,L}$ by 35.52 ± 2.93% at EDS (control: −7.32 ± 0.46 pA/pF, $n = 8$; OA: −9.92 ± 0.82 pA/pF, $n = 8$, $P < 0.05$) but increased $I_{Ca,L}$ only by 17.11 ± 2.19% at LDS (control: −16.25 ± 1.34 pA/pF, $n = 10$; OA: −19.03 ± 2.44 pA/pF, $n = 10$, $P < 0.05$), which suggested a higher PP1/PP2A activity at EDS than LDS.

3.4. Calcium-channel gating under basal conditions and effects of 8-Br-cAMP on LTCC gating

As expected, single-channel activity of LTCCs was substantially higher in EDS than LDS cardiomyocytes, as illustrated by original recordings (Fig. 5B) and by the corresponding open-time and closed-time histograms (Fig. 5D). The larger ensemble average current (Fig. 5C) was due to both the higher availability and the higher open probability. The latter effect was caused predominantly by the shorter closed times (Fig. 5D). Details are listed in Table 2, where a higher open probability of channels at EDS was observed due to the shorter first latency, the longer mean open time, and the shorter closed time (faster time constant of the slow component). The unitary current amplitude i was similar (P = NS) between the two groups. Importantly, single-channel conductance, obtained by measuring the amplitudes of fully resolved openings at +20 mV, was identical (P = NS) between channels from EDS (23.6 ± 2.2 pS, $n = 9$) and LDS (23.5 ± 1.8 pS, $n = 11$) cardiomyocytes.

The higher baseline open probability and availability at EDS could not be increased by stimulation of 8-Br-cAMP (Table 3). However, the experiments with cells from LDS cardiomyocytes showed a strong increase in current (from 12 ± 3 to 46 ± 9 fA, $n = 7$; $P < 0.01$) (Table 3). This raises the idea that a phosphorylation-related

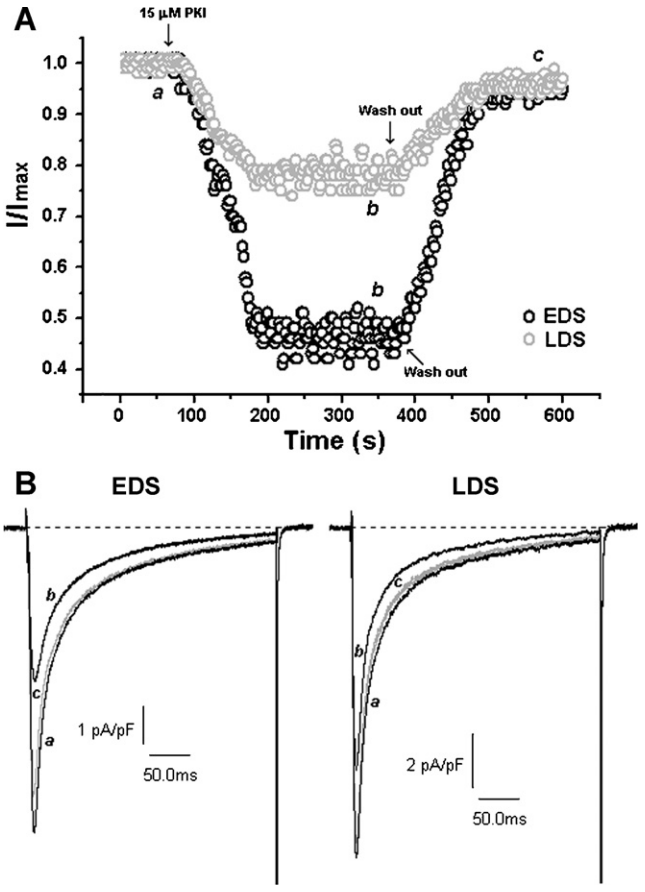

Fig. 4. Effects of 15 μmol/L PKI on $I_{Ca,L}$ in EDS and LDS cardiomyocytes. (A) Time course of the effects of exposure to PKI in EDS and LDS cardiomyocytes. Data plotted in the figure are mean (EDS: $n = 6$ cells from 4 hearts; LDS: $n = 6$ cells from 3 hearts) peak inward current amplitudes normalized to initial current values (I/I_{max}) in EDS and LDS cardiomyocytes. Currents were recorded in response to repetitive application (0.5 Hz) of 300 ms pulses to 0 mV from −40 mV holding potentials. (B) Representative current traces recorded in individual EDS and LDS cells before, after application of PKI and washout of the drug at times indicated in A.

Table 2
Comparison of single-channel properties of L-type calcium channels in EDS and LDS cardiomyocytes.

Parameter	EDS	*n*	LDS	*n*
Open probability (%)	9.63 ± 1.45	9	2.80 ± 1.12**	12
Availability (%)	61.2 ± 4.2	11	33.6 ± 2.7*	12
Mean first latency (ms)	37.3 ± 3.57	8	49.7 ± 4.48*	12
Mean open time (ms)	0.57 ± 0.04	9	0.42 ± 0.05*	12
τ_{open} (ms)	0.55 ± 0.03	9	0.40 ± 0.04*	12
Mean closed time (ms)	2.86 ± 0.53	8	19.3 ± 4.71**	9
$\tau_{closed,fast}$ (ms)	0.51 ± 0.03	8	0.72 ± 0.05	9
$\tau_{closed,slow}$ (ms)	13.57 ± 1.16	8	20.6 ± 1.1*	9
Fraction $\tau_{closed,fast}$	0.48 ± 0.06	8	0.49 ± 0.07	9
Amplitude (pA)	−0.67 ± 0.06	10	−0.65 ± 0.05	11
I_{peak} (fA)	27.5 ± 9	10	14.0 ± 6*	11

Unitary single-channel amplitude, from amplitude histogram; for closed times and latency analysis, only patches containing one single channel were used. The other values were corrected for the number of channels present. EDS cardiomyocytes were from 4 different embryonic hearts, and LDS cardiomyocytes were from 6 different embryonic hearts. Values are expressed as mean ± SEM.

* $P < 0.05$ versus EDS group.

** $P < 0.01$ versus EDS group.

Table 3
Effects of 8-Br-cAMP on single-channel behavior.

Parameter and group	Control	8-Br-cAMP (1 mM)	*n*
Open probability (%)			
EDS	12.1 ± 2.47	14.5 ± 3.29	8
LDS	2.2 ± 1.16	12.6 ± 1.97**	11
Availability (%)			
EDS	58.7 ± 8.4	65.5 ± 8.3	8
LDS	35.3 ± 3.1	59.3 ± 5.5*	11
Mean first latency (ms)			
EDS	38.2 ± 5.5	34.9 ± 6.1	7
LDS	51.3 ± 6.0	35.7 ± 4.5*	10
Mean open time (ms)			
EDS	0.58 ± 0.07	0.62 ± 0.04	6
LDS	0.45 ± 0.05	0.55 ± 0.06*	8
τ_{open} (ms)			
EDS	0.60 ± 0.09	0.60 ± 0.11	6
LDS	0.44 ± 0.07	0.52 ± 0.08*	8
Mean closed time (ms)			
EDS	2.97 ± 0.75	2.72 ± 0.83	6
LDS	17.9 ± 5.24	11.3 ± 4.85*	9
$\tau_{closed,fast}$ (ms)			
EDS	0.46 ± 0.05	0.41 ± 0.06	6
LDS	0.84 ± 0.09	0.77 ± 0.08	9
$\tau_{closed,slow}$ (ms)			
EDS	9.81 ± 1.23	9.54 ± 1.47	6
LDS	18.6 ± 1.54	14.3 ± 1.60*	9
Amplitude (pA)			
EDS	−0.69 ± 0.04	−0.67 ± 0.05	5
LDS	−0.67 ± 0.05	−0.68 ± 0.06	8
I_{peak} (fA)			
EDS	28 ± 7	32 ± 11	5
LDS	12 ± 3	46 ± 9**	7

Thirteen single-channel patches and 6 double-channel patches were recorded from cells of 9 hearts, 4 EDS and 5 LDS hearts. Values are expressed as mean ± SEM.

* $P < 0.05$ versus control group.

** $P < 0.01$ versus control group.

mechanism is responsible for the higher activity of channels in cardiomyocytes derived from EDS as compared to LDS.

3.5. Effects of PKI and OA on LTCC gating

Our data showed that the peak current (Fig. 6A), the availability (Fig. 6B) and the open probability (Fig. 6C) were significantly decreased after PKI (15 μmol/L) was administrated. However, PKI effects on the peak current (decreased by 55.7 ± 7.2%, $P < 0.01$, $n = 6$, EDS; decreased by 26.7 ± 4.5%, $P < 0.05$, $n = 8$, LDS), the open probability (decreased by 54.4 ± 7.6%, $P < 0.01$, $n = 6$, EDS; decreased by 40.2 ± 6.5%, $P < 0.05$, $n = 8$, LDS) and the availability (decreased by 53.0 ± 6.7%, $P < 0.05$, $n = 6$, EDS; decreased by 37.2 ± 5.8%, $P < 0.05$, $n = 8$, LDS) were greater in myocytes at EDS than LDS (Fig. 6A–C). Consistent with the whole cell recordings, OA (10 μmol/L) exerted greater effects at EDS than LDS on the peak current and the open probability (Fig. 6 D and E). Availability, known to be regulated by phosphatase 1 [44,45], also increased slightly in both groups (Fig. 6F), indicating that there is no difference in phosphatase 1.

3.6. Phosphorylation of $\alpha_1$1.2 during development

Phospho-specific antibody anti-CH3P against phosphorylated serine 1928 was probed by immunoblotting analysis of $Ca_v1.2$ channels in fetal ventricular cardiomyocytes. The expression of $\alpha_1$1.2 increases with development (data not shown). To determine whether this site was phosphorylated by stimulation of PKA in vivo, ISO was used to activate PKA. After ISO treatment, there were no significant differences in the level of phosphorylated serine 1928 between these two groups (Fig. 7A). However, the basal phosphorylation level of serine 1928 was obviously higher at EDS than LDS (Fig. 7). Thus, phosphorylation of $\alpha_1$1.2 on serine 1928 and, thereby, channel activity, is significantly higher at EDS than LDS (Fig. 5B).

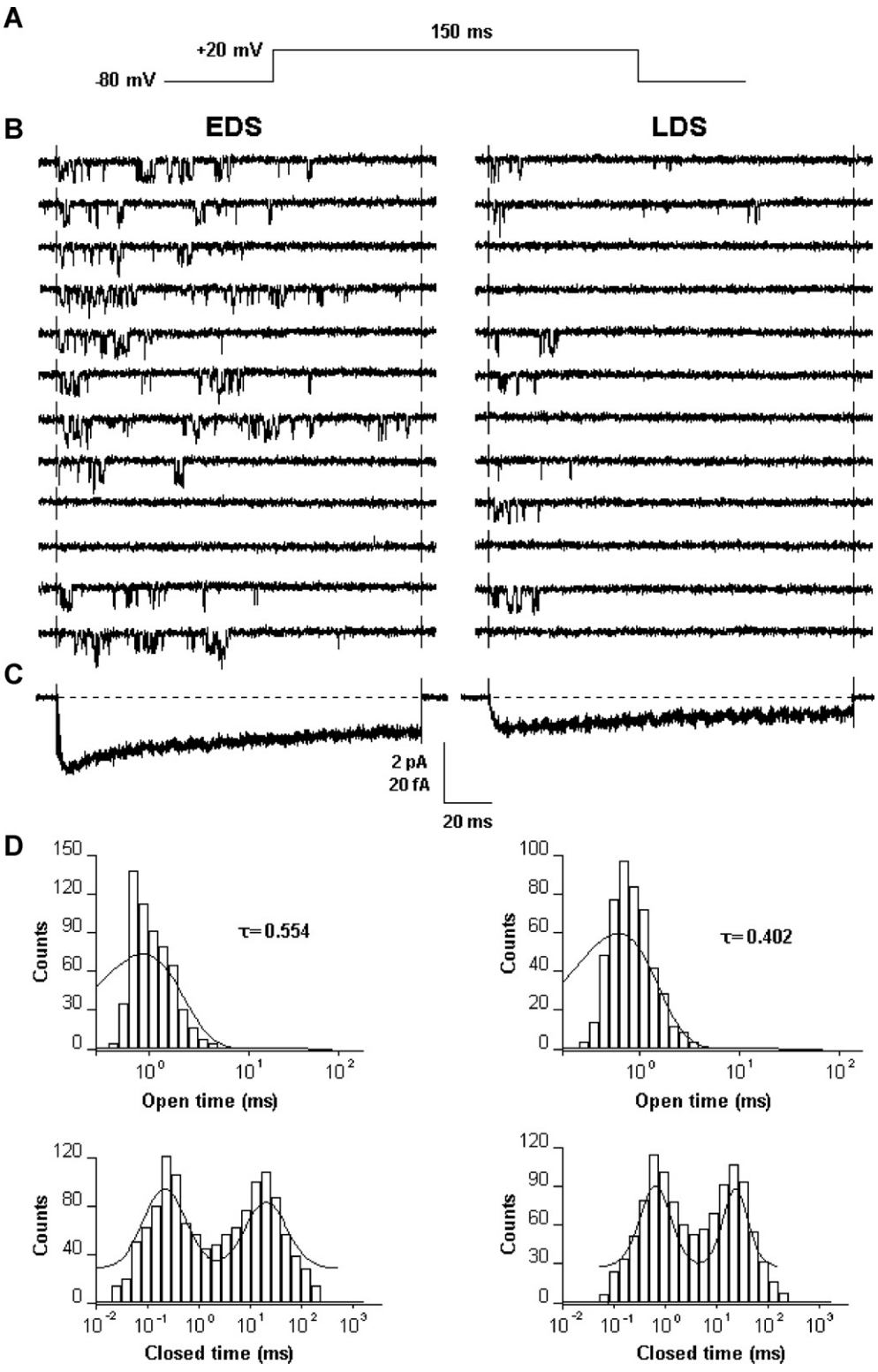

Fig. 5. Comparison of single L-type calcium channels in EDS (left) and LDS (right) cardiomyocytes. (A) Voltage protocol. (B) Consecutive sweeps. (C) Average current of all 200 (left) or 240 (right) sweeps of entire ensembles. (D) Open time (top) and closed time (bottom) histograms of two experiments. Curves were generated with a maximum-likelihood estimate for simple (open times) or double exponential (closed times). Time constants amounted to τ_{open} = 0.55 ms, $\tau_{closed,fast}$ = 0.51 ms, and $\tau_{closed,slow}$ = 13.57 ms for channel from EDS cardiomyocytes and τ_{open} = 0.40 ms, $\tau_{closed,fast}$ = 0.72 ms, and $\tau_{closed,slow}$ = 20.6 ms for channel from LDS cardiomyocytes.

3.7. cAMP concentration, AC activity and effects of Ca^{2+} buffering on Ca^{2+} current

To determine whether the cAMP concentration was higher at EDS as compared to LDS, we measured the cAMP concentration in ventricular cardiomyocytes with or without the application of following drugs. The basal cAMP concentration was substantially higher in EDS than LDS cardiomyocytes and was markedly suppressed by AC inhibitor MDL-12,330A (Fig. 8A, left panel). At EDS, 400 μmol/L MDL-12,330A produced a more profound decrease

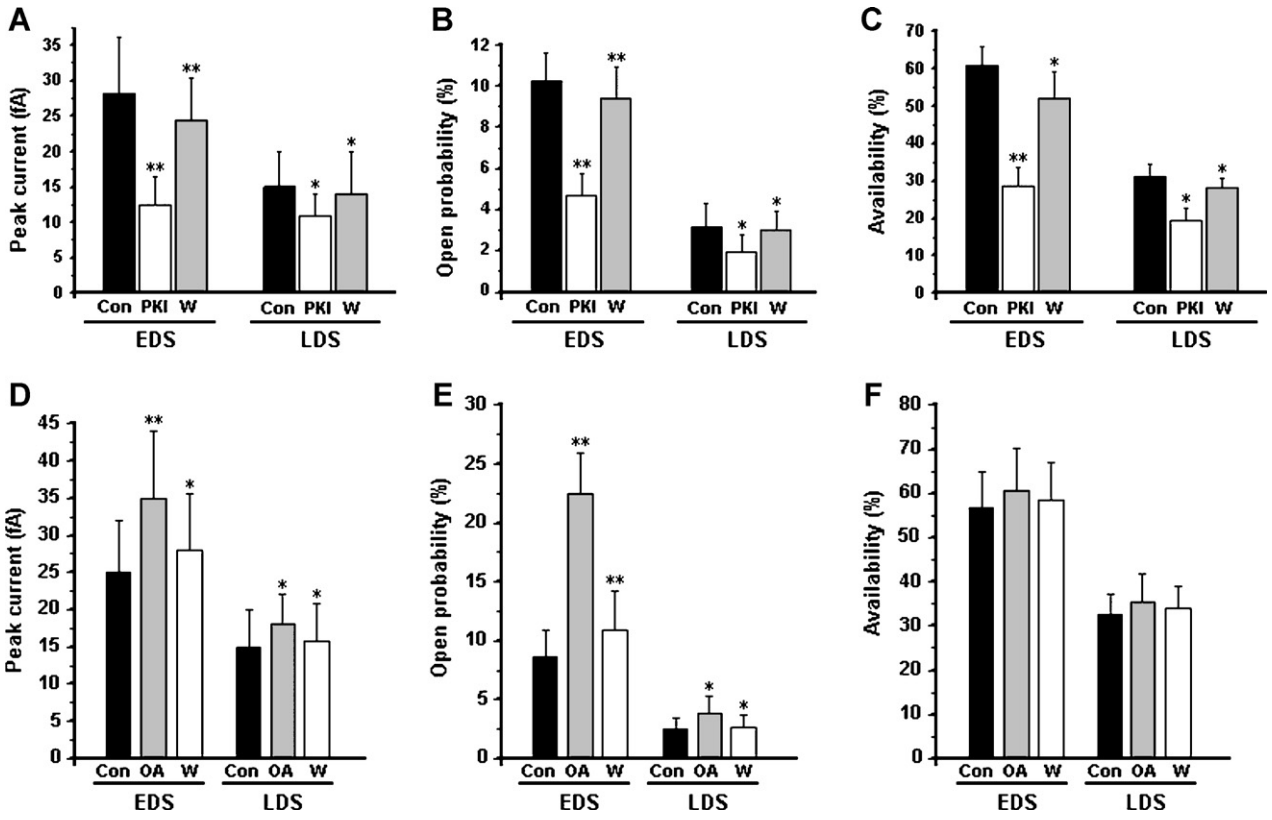

Fig. 6. Effects of PKI or Okadaic Acid on Ba^{2+} currents through single L-type Ca^{2+} channels recorded in EDS (PKI, $n=6$ cells from 4 hearts; Okadaic Acid, $n=7$ cells from 4 hearts) and LDS (PKI, $n=8$ cells from 4 hearts; Okadaic Acid, $n=7$ cells from 5 hearts) cardiomyocytes. Drug effects on peak average current (A, D), channel availability (B, E) and open probability (C, F) are depicted with respective controls. Data are presented as mean ± SEM. $^{**}P<0.01$, $^{*}P<0.05$. Abbreviations: Con, control; OA, Okadaic Acid; W, Washout.

(52.9 ± 6.2%, $P<0.01$) in the cAMP concentration than that at LDS (25.7 ± 4.5% reduction) ($P<0.05$). The cAMP level was markedly affected by PDE inhibitor IBMX. At EDS, 100 μmol/L IBMX had a stronger effect on the cAMP concentration (about 3.5-fold) than that at LDS (about 2.8-fold), suggesting a higher level of AC activity (Fig. 8A, right panel).

Our results provide direct evidence, in whole cell lysates of intact embryonic cardiomyocytes, of Ca^{2+}-inhibited AC activity in the absence of sucrose density cell fractioning. Following incubation of whole cell lysates in Ca^{2+}-free buffer containing EGTA, AC activity was greatly decreased by incubation in the presence of Ca^{2+} at concentrations that occur within the physiologic range in EDS and LDS cells (Fig. 8C, left panel). Since the Ca^{2+}-inhibitable isoforms AC5 and AC6 are the most abundant in the heart, BAPTA-AM was applied to evaluate contribution of AC5 and AC6. The basal AC activity was markedly enhanced at LDS but not at EDS by chelation of intracellular Ca^{2+} with BAPTA-AM (Fig. 8C, right panel). Furthermore, in the presence of IBMX, cAMP concentration further augmented at LDS but not at EDS by application of BAPTA-AM (Fig. 8A, right panel). Meanwhile, $I_{Ca,L}$ increased with time after dialyzed with pipette solution containing BAPTA in LDS whereas not in EDS cardiomyocytes (data not shown). As seen in Fig. 8B, 40 mM BAPTA had only minor effects (+5.4 ± 2.4%) on $I_{Ca,L}$ amplitude at EDS ($n=7$; P = NS), whereas it strongly stimulated $I_{Ca,L}$ at LDS (+39.3 ± 6.2%, $n=7$; $P<0.05$). This suggests that at EDS the high activity of LTCCs is probably due to "Ca^{2+} has little influence on AC activity", and at LDS the stimulation of $I_{Ca,L}$ in BAPTA probably results from chelation of Ca^{2+} that disinhibits AC, leading to increase of a local cAMP (Fig. 8A, right panel).

4. Discussion

In the present study, we investigated the regulation of LTCCs in murine embryonic ventricles. The electrophysiological findings

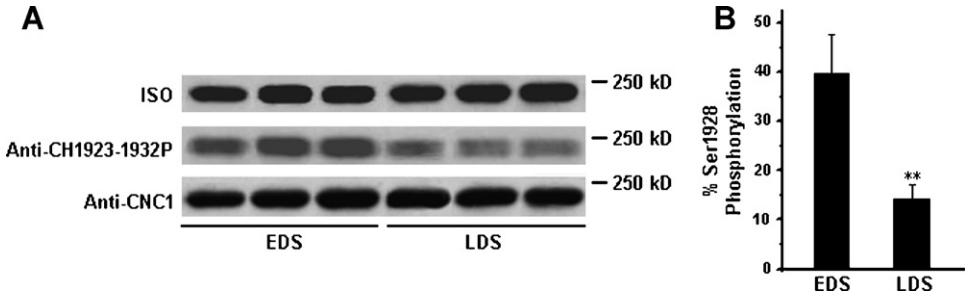

Fig. 7. Phosphorylation of serine 1928 in the α_1 subunit of $Ca_V1.2$ channels in embryonic ventricular cardiomyocytes. (A) Immunoblotting to detect both basal and ISO-induced phosphorylation of $\alpha_1$1.2 on serine 1928. (B) Normalized basal phosphorylation of $\alpha_1$1.2 on serine 1928 (normalized to $\alpha_1$1.2) in EDS and LDS cardiomyocytes. Data were obtained from 4 to 6 independent protein preparations. $^{**}P<0.01$, EDS versus LDS.

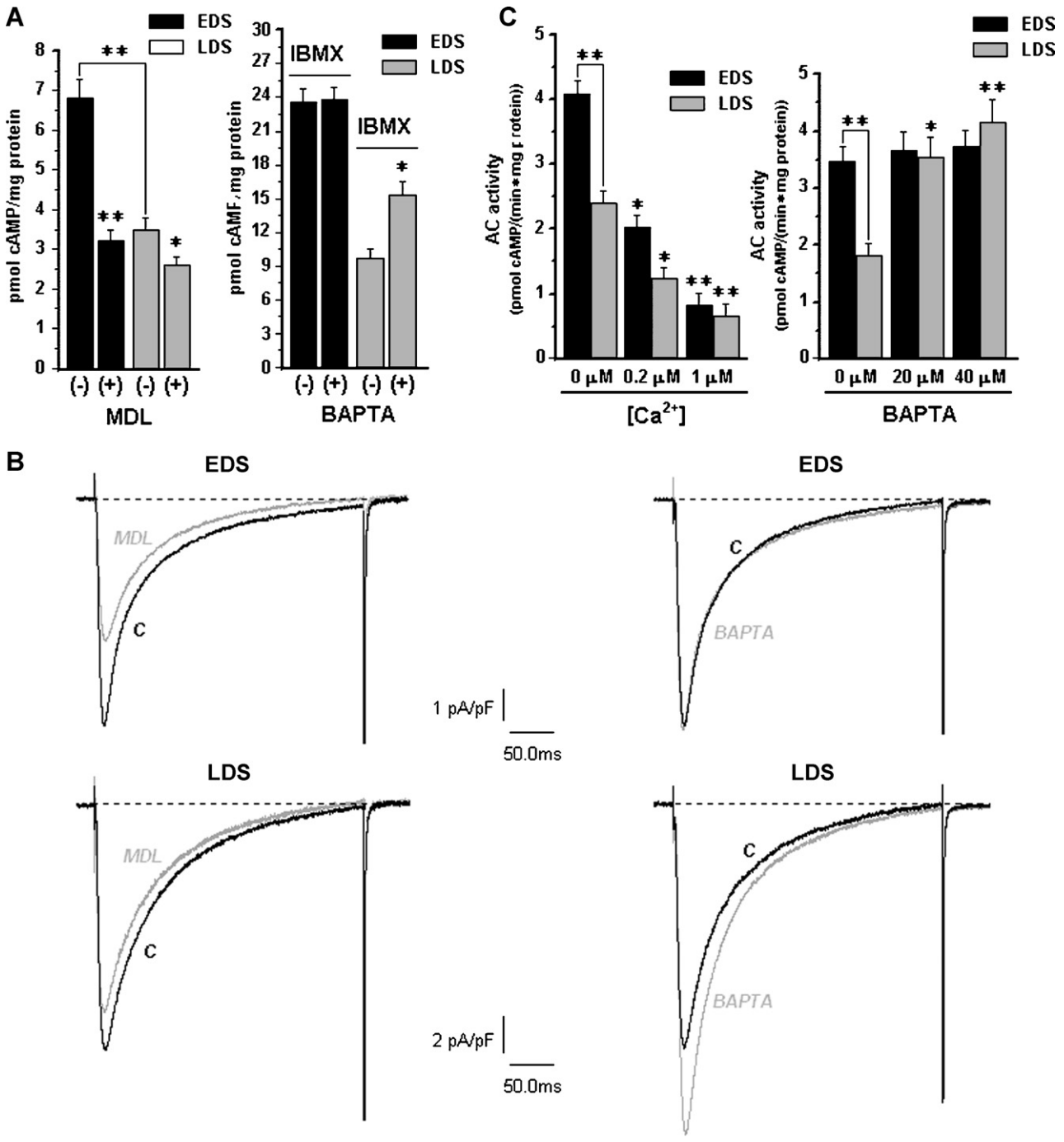

Fig. 8. Effects of MDL-12,330A, intracellular Ca^{2+}-chelating compounds on total cellular cAMP levels (or AC activity) and $I_{Ca,L}$ in EDS and LDS cardiomyocytes. (A) Total cellular cAMP levels following adenylyl cyclase (AC) inhibition; phosphodiesterase inhibition, or a combination of both, in the presence (+) or absence (−) of chelation of intracellular Ca^{2+} by BAPTA-AM. (B) Effects of MDL-12,330A, BAPTA on $I_{Ca,L}$. C: control; MDL: MDL-12,330A; BAPTA: BAPTA-AM. (C) Effects of Ca^{2+} and BAPTA-AM on AC activity in EDS and LDS cardiomyocytes.

together with our biochemical evidence demonstrated that a higher phosphorylation state of LTCC at EDS as compared to LDS. The whole-cell recordings provided three independent observations to confirm this finding: (1) the leftward shift of $I_{Ca,L}$–V curves in EDS cardiomyocytes under basal condition but unaffected $I_{Ca,L}$–V curves after ISO and 8-Br-cAMP application; (2) smaller effects of ISO and 8-Br-cAMP on $I_{Ca,L}$ at EDS; and (3) stronger effects of PKI, H-89 on peak $I_{Ca,L}$ in EDS cardiomyocytes. Cell-attached recordings also provided three independent observations consistent with a higher phosphorylation state of LTCC in EDS than LDS cardiomyocytes: (1) the higher activity of channels at EDS under basal condition which resembled the pattern of cAMP-dependent stimulation of cardiac LTCCs known from animal experiments; (2) smaller effects of 8-Br-cAMP on LTCC gating in EDS cardiomyocytes; and (3) greater effects of PKI on LTCC gating at EDS.

The whole-cell current I is a function of both the number of functional channels N and their individual properties i (single-channel current amplitude), the open probability (p_{open}, fraction of time spent in the open state during active sweeps), and the availability (f_{active}, fraction of active sweeps per number of test pulses), where $I = N \times i \times p_{open} \times f_{active}$ [40]. However, our cell-attached recordings showed the unitary current amplitude i was similar (P = NS)

between channels from EDS and LDS cardiomyocytes. Therefore, I is determined by alterations of N, p_{open}, or f_{active}. Although p_{open}, and f_{active} were substantially higher in EDS than LDS cardiomyocytes, depolarization possibly activated more L-type calcium channels (N), which was contributing to the higher $I_{Ca,L}$ density at more depolarized potentials at LDS. It is reported that the increase of N mainly contributes to the increase of $I_{Ca,L}$ density during embryonic heart development [20]. Therefore, at less depolarized potential larger $I_{Ca,L}$ was recorded owing to higher p_{open}, and f_{active}. More depolarized potentials activated more L-type calcium channels in LDS cardiomyocytes thus the whole cell current density was higher.

The whole-cell recordings suggested that a negative shift in the voltage dependence of $I_{Ca,L}$ activation could be induced by a higher basal level of LTCC phosphorylation in EDS than LDS cardiomyocytes. This idea was consistent with the higher open probability of single LTCCs at EDS, a behavior caused by channel phosphorylation. In EDS cardiomyocytes, the high intrinsic activity of AC (Fig. 8A, right panel and Fig. 8C) might contribute to the high cAMP level (Fig. 8A, left panel) thereafter for the high PKA activity (Figs. 4 and 6) and the high basal LTCC activity.

As a PKA phosphorylation site, serine 1928 had important implications regarding the study of phosphorylation-dependent modulation of $Ca_v1.2$ [46,47]. The immunoblot analysis in the present study provided direct evidence that the basal phosphorylation level of serine 1928 was obviously higher at EDS than LDS (Fig. 7B).

EDS cells were characterized by a high intrinsic AC activity (Fig. 8C), which was confirmed by the effect of MDL-12,330A, an AC inhibitor (Fig. 8A, left panel). The high intrinsic AC activity could relate to AC expression, or modulation by differences in resting Ca^{2+} and/or G-protein. In fact, previous studies have shown that the level of AC6 mRNA decreased with age, paralleling the decline in the functional activity of AC with age [48]. In the heart, an elevation of Ca^{2+} entry via LTCCs, rather than its release from intracellular stores, may mediate its inhibition of AC5 and AC6 and act as a negative regulator of the receptor-mediated AC activity [49]. This inhibition could provide a feedback in situations where cAMP promotes opening of Ca^{2+} channels, allowing fine control of cardiac contraction in cardiac tissue where AC5 and AC6 predominate [50]. The Ca^{2+} close to LTCC entry sites seems to be responsible for the modulation of Ca^{2+}-sensitive AC activity [33]. In contrast to LDS cells and adult murine ventricular cardiomyocytes [33,34,50], the low $I_{Ca,L}$ density at EDS might allow less submembrane free Ca^{2+} concentration in the vicinity of the Ca^{2+} channel pore (Ca_{sm}^{2+}) [51,52], thereby basal resting free Ca^{2+} had little influence on AC activity in EDS cells (Fig. 8B and C, right panel). Furthermore, it had originally been observed that AC5, and AC6 were inhibited by G_i [53], which could mediated lowering of AC activity in LDS but not EDS cardiomyocytes [25]. It may also account for the high AC activity at EDS.

A high basal PDE activity in EDS cardiomyocytes has recently been demonstrated [21]. The present results showed that both Ca^{2+}-inhibited AC activity and PDE activity (Fig. 8A, right panel) regulate basal cAMP levels in EDS cardiomyocytes. A high basal AC activity coupled to high PDE activity created continuous cAMP synthesis and degradation. It has been proposed that restricting such continuous cAMP production and degradation to subcellular components would be an energetically efficient way to allow a system (e.g. cyclic nucleotide-gated channels [54]) to respond rapidly to a stimulus.

Surprisingly, both whole-cell and single-channel data indicated high intrinsic phosphatase activity in EDS cardiomyocytes. And the pattern of single channel gating and the strong effect of okadaic acid on open probability at EDS indicated a great influence of phosphatase 2A (PP2A) on LTCCs particularly. In cardiac tissues, protein phosphatase 2A (PP2A) has been identified as one of the major phosphatases associated with protein contraction machinery [55,56]. It is reported that both PKA and PP2A are integral components of the LTCC that determine the phosphorylation level of serine 1928 and channel activity [57]. Phosphatases are often associated with scaffold protein A kinase anchoring proteins (AKAPs), which also anchor PKA holoenzymes [58]. Previous research has shown that PP2A is activated by a cAMP/PKA-dependent pathway, leading to dephosphorylation of Thr-75 [59]. The locally bound PKA and phosphatase thus act together for tight regulation on phosphorylation of substrates [60]. Under our conditions the basal phosphorylation state of LTCCs is determined by activities of PKA and phosphatases [57,61]. However, a high level of endogenous PKA activity might outweigh the endogenous phosphatase activity, hence the basal level of LTCC phosphorylation is higher in cardiomyocytes derived from EDS as compared to LDS.

Our study gives a novel insight into the mechanisms responsible for PKA activity that exists in the absence of β-adrenergic receptor stimulation. This could be important in the context of heart failure, where alterations in basal phosphorylation of LTCCs, perhaps due to changes in phosphatase activity [40,62,63], could contribute to the pathogenesis of the disease.

Acknowledgements

The authors thank Liangzhu Yu, Aifen Liu, and Ying Cheng for help in cell culture work. We are also grateful to Li Nie and Xiongfei Zhao for helping with the Patch clamp experiments and Meilin Tang for advice with ELISA. This work is supported by two grants from National Nature Science Foundation of China NSFC grant (No. 30700262 for Huamin Liang and No. 30670854 for Linlin Gao), a Ph.D. Program Foundation of Ministry of Education of China for Ming Tang (No. 20070487012), and two grants assisted by Science Foundation of Huazhong University of Science and Technology (No. 0109510022 for Jiaoya Xi and No. 012551 for Yunjie Zheng).

References

[1] H. Reuter, Calcium channel modulation by neurotransmitters, enzymes and drugs, Nature 301 (1983) 569–574.
[2] T.F. McDonald, S. Pelzer, W. Trautwein, D.J. Pelzer, Regulation and modulation of calcium channels in cardiac, skeletal, and smooth muscle cells, Physiol. Rev. 74 (1994) 365–507.
[3] W.C. Lester, E.A. Schroder, D.E. Burgess, D. Yozwiak, D.A. Andres, J. Satin, Steady-state coupling of plasma membrane calcium entry to extrusion revealed by novel L-type calcium channel block, Cell Calcium 44 (2008) 353–362.
[4] F. Swift, N. Tovsrud, I. Sjaastad, O.M. Sejersted, E. Niggli, M. Egger, Functional coupling of alpha(2)-isoform Na^+/K^+-ATPase and Ca^{2+} extrusion through the Na^+/Ca^{2+}-exchanger in cardiomyocytes, Cell Calcium 48 (2010) 54–60.
[5] J.D. Turner, A.P. Thomas, J.P. Reeves, B.M. Hantash, Calcineurin activation by slow calcium release from intracellular stores suppresses protein kinase C regulation of L-type calcium channels in L6 cells, Cell Calcium 46 (2009) 242–247.
[6] W. Trautwein, J. Hescheler, Regulation of cardiac L-type calcium current by phosphorylation and G proteins, Annu. Rev. Physiol. 52 (1990) 257–274.
[7] J.P. Benitah, J.L. Alvarez, A.M. Gomez, L-type Ca^{2+} current in ventricular cardiomyocytes, J. Mol. Cell. Cardiol. 48 (2010) 26–36.
[8] A. Yatani, Y. Tajima, S.A. Green, Coupling of beta-adrenergic receptors to cardiac L-type Ca^{2+} channels: preferential coupling of the beta(1) versus beta(2) receptor subtype and evidence for PKA-independent activation of the channel, Cell. Signal. 11 (1999) 337–342.
[9] M.A. Brotto, T.L. Creazzo, Ca^{2+} transients in embryonic chick heart: contributions from Ca^{2+} channels and the sarcoplasmic reticulum, Am. J. Physiol. 270 (1996) H518–H525.
[10] V. Ramesh, M.J. Kresch, A.M. Katz, D.H. Kim, Characterization of Ca^{2+}-release channels in fetal and adult rat hearts, Am. J. Physiol. 269 (1995) H778–H782.
[11] J.K. Larsen, J.W. Mitchell, P.M. Best, Quantitative analysis of the expression and distribution of calcium channel alpha 1 subunit mRNA in the atria and ventricles of the rat heart, J. Mol. Cell. Cardiol. 34 (2002) 519–532.
[12] E.A. Ertel, K.P. Campbell, M.M. Harpold, F. Hofmann, Y. Mori, E. Perez-Reyes, A. Schwartz, T.P. Snutch, T. Tanabe, L. Birnbaumer, R.W. Tsien, W.A. Catterall, Nomenclature of voltage-gated calcium channels, Neuron 25 (2000) 533–535.
[13] A. Mikami, K. Imoto, T. Tanabe, T. Niidome, Y. Mori, H. Takeshima, S. Narumiya, S. Numa, Primary structure and functional expression of the cardiac dihydropyridine-sensitive calcium channel, Nature 340 (1989) 230–233.
[14] A. Sculptoreanu, E. Rotman, M. Takahashi, T. Scheuer, W.A. Catterall, Voltage-dependent potentiation of the activity of cardiac L-type calcium channel alpha

1 subunits due to phosphorylation by cAMP-dependent protein kinase, Proc. Natl. Acad. Sci. U. S. A. 90 (1993) 10135–10139.
[15] M.A. van der Heyden, T.J. Wijnhoven, T. Opthof, Molecular aspects of adrenergic modulation of cardiac L-type Ca^{2+} channels, Cardiovasc. Res. 65 (2005) 28–39.
[16] T.J. Kamp, J.W. Hell, Regulation of cardiac L-type calcium channels by protein kinase A and protein kinase C, Circ. Res. 87 (2000) 1095–1102.
[17] L. Yang, G. Liu, S.I. Zakharov, J.P. Morrow, V.O. Rybin, S.F. Steinberg, S.O. Marx, Ser1928 is a common site for $Ca_v1.2$ phosphorylation by protein kinase C isoforms, J. Biol. Chem. 280 (2005) 207–214.
[18] K.S. De Jongh, B.J. Murphy, A.A. Colvin, J.W. Hell, M. Takahashi, W.A. Catterall, Specific phosphorylation of a site in the full-length form of the alpha 1 subunit of the cardiac L-type calcium channel by adenosine 3′,5′-cyclic monophosphate-dependent protein kinase, Biochemistry 35 (1996) 10392–10402.
[19] F. Nguemo, P. Sasse, B.K. Fleischmann, A. Kamanyi, H. Schunkert, J. Hescheler, M. Reppel, Modulation of L-type Ca^{2+} channel current density and inactivation by beta-adrenergic stimulation during murine cardiac embryogenesis, Basic Res. Cardiol. 104 (2009) 295–306.
[20] F. Nguemo, B.K. Fleischmann, H. Schunkert, J. Hescheler, M. Reppel, Functional expression and inactivation of L-type Ca^{2+} currents during murine heart development-implications for cardiac Ca^{2+} homeostasis, Cell. Physiol. Biochem. 20 (2007) 809–824.
[21] V.A. Maltsev, G.J. Ji, A.M. Wobus, B.K. Fleischmann, J. Hescheler, Establishment of beta-adrenergic modulation of L-type Ca^{2+} current in the early stages of cardiomyocyte development, Circ. Res. 84 (1999) 136–145.
[22] T.M. Vinogradova, S. Sirenko, A.E. Lyashkov, A. Younes, Y. Li, W. Zhu, D. Yang, A.M. Ruknudin, H. Spurgeon, E.G. Lakatta, Constitutive phosphodiesterase activity restricts spontaneous beating rate of cardiac pacemaker cells by suppressing local Ca^{2+} releases, Circ. Res. 102 (2008) 761–769.
[23] E. Patrucco, M.S. Albergine, L.F. Santana, J.A. Beavo, Phosphodiesterase 8A (PDE8A) regulates excitation–contraction coupling in ventricular myocytes, J. Mol. Cell. Cardiol. 49 (2010) 330–333.
[24] H. Wang, M.J. Kohr, C.J. Traynham, M.T. Ziolo, Phosphodiesterase 5 restricts NOS3/Soluble guanylate cyclase signaling to L-type Ca^{2+} current in cardiac myocytes, J. Mol. Cell. Cardiol. 47 (2009) 304–314.
[25] G.J. Ji, B.K. Fleischmann, W. Bloch, M. Feelisch, C. Andressen, K. Addicks, J. Hescheler, Regulation of the L-type Ca^{2+} channel during cardiomyogenesis: switch from NO to adenylyl cyclase-mediated inhibition, FASEB J. 13 (1999) 313–324.
[26] M.L. Bayewitch, T. Avidor-Reiss, R. Levy, T. Pfeuffer, I. Nevo, W.F. Simonds, Z. Vogel, Inhibition of adenylyl cyclase isoforms V and VI by various Gbetagamma subunits, FASEB J. 12 (1998) 1019–1025.
[27] D.M. Cooper, N. Mons, J.W. Karpen, Adenylyl cyclases and the interaction between calcium and cAMP signalling, Nature 374 (1995) 421–424.
[28] S. Herzig, J. Neumann, Effects of serine/threonine protein phosphatases on ion channels in excitable membranes, Physiol. Rev. 80 (2000) 173–210.
[29] W.H. duBell, M.S. Gigena, S. Guatimosim, X. Long, W.J. Lederer, T.B. Rogers, Effects of PP1/PP2A inhibitor calyculin A on the E-C coupling cascade in murine ventricular myocytes, Am. J. Physiol. Heart Circ. Physiol. 282 (2002) H38–H48.
[30] W.H. duBell, T.B. Rogers, Protein phosphatase 1 and an opposing protein kinase regulate steady-state L-type Ca^{2+} current in mouse cardiac myocytes, J. Physiol. 556 (2004) 79–93.
[31] G.L. Song, M. Tang, C.J. Liu, H.Y. Luo, H.M. Liang, X.W. Hu, J.Y. Xi, L.L. Gao, B. Fleischmann, J. Hescheler, Developmental changes in functional expression and beta-adrenergic regulation of I(f) in the heart of mouse embryo, Cell Res. 12 (2002) 385–394.
[32] B.K. Fleischmann, Y. Duan, Y. Fan, T. Schoneberg, A. Ehlich, N. Lenka, S. Viatchenko-Karpinski, L. Pott, J. Hescheler, B. Fakler, Differential subunit composition of the G protein-activated inward-rectifier potassium channel during cardiac development, J. Clin. Invest. 114 (2004) 994–1001.
[33] Y. You, D.J. Pelzer, S. Pelzer, Modulation of L-type Ca^{2+} current by fast and slow Ca^{2+} buffering in guinea pig ventricular cardiomyocytes, Biophys. J. 72 (1997) 175–187.
[34] J.B. Shen, A.J. Pappano, Carbachol inhibits the L-type Ca^{2+} current augmented by 1,2-bis(2-aminophenoxy)ethane-N,N,N′,N′-tetraacetic acid in guinea pig ventricular myocytes: calcium-sensitivity hypothesis for muscarinic inhibition, J. Pharmacol. Exp. Ther. 298 (2001) 857–864.
[35] S. Adachi-Akahane, L. Cleemann, M. Morad, Cross-signaling between L-type Ca^{2+} channels and ryanodine receptors in rat ventricular myocytes, J. Gen. Physiol. 108 (1996) 435–454.
[36] S.I. McDonough, Y. Mori, B.P. Bean, FPL 64176 modification of $Ca_V1.2$ L-type calcium channels: dissociation of effects on ionic current and gating current, Biophys. J. 88 (2005) 211–223.
[37] D.M. Bers, C.W. Patton, R. Nuccitelli, A practical guide to the preparation of Ca^{2+} buffers, Methods Cell Biol. 40 (1994) 3–29.
[38] P. Narayan, R.M. Mentzer Jr., R.D. Lasley, Phosphatase inhibitor cantharidin blocks adenosine A(1) receptor anti-adrenergic effect in rat cardiac myocytes, Am. J. Physiol. Heart Circ. Physiol. 278 (2000) H1–H7.
[39] A. Younes, A.E. Lyashkov, D. Graham, A. Sheydina, M.V. Volkova, M. Mitsak, T.M. Vinogradova, Y.O. Lukyanenko, Y. Li, A.M. Ruknudin, K.R. Boheler, J. van Eyk, E.G. Lakatta, Ca^{2+}-stimulated basal adenylyl cyclase activity localization in membrane lipid microdomains of cardiac sinoatrial nodal pacemaker cells, J. Biol. Chem. 283 (2008) 14461–14468.
[40] F. Schroder, R. Handrock, D.J. Beuckelmann, S. Hirt, R. Hullin, L. Priebe, R.H. Schwinger, J. Weil, S. Herzig, Increased availability and open probability of single L-type calcium channels from failing compared with nonfailing human ventricle, Circulation 98 (1998) 969–976.
[41] G. Klein, F. Schroder, D. Vogler, A. Schaefer, A. Haverich, B. Schieffer, T. Korte, H. Drexler, Increased open probability of single cardiac L-type calcium channels in patients with chronic atrial fibrillation. role of phosphatase 2A, Cardiovasc. Res. 59 (2003) 37–45.
[42] G. Michels, J. Matthes, R. Handrock, U. Kuchinke, F. Groner, L.L. Cribbs, A. Pereverzev, T. Schneider, E. Perez-Reyes, S. Herzig, Single-channel pharmacology of mibefradil in human native T-type and recombinant $Ca_v3.2$ calcium channels, Mol. Pharmacol. 61 (2002) 682–694.
[43] K.B. Walsh, T.B. Begenisich, R.S. Kass, Beta-adrenergic modulation of cardiac ion channels. Differential temperature sensitivity of potassium and calcium currents, J. Gen. Physiol. 93 (1989) 841–854.
[44] K. Wiechen, D.T. Yue, S. Herzig, Two distinct functional effects of protein phosphatase inhibitors on guinea-pig cardiac L-type Ca^{2+} channels, J. Physiol. 484 (Pt 3) (1995) 583–592.
[45] K. Ono, H.A. Fozzard, Two phosphatase sites on the Ca^{2+} channel affecting different kinetic functions, J. Physiol. 470 (1993) 73–84.
[46] T. Lemke, A. Welling, C.J. Christel, A. Blaich, D. Bernhard, P. Lenhardt, F. Hofmann, S. Moosmang, Unchanged beta-adrenergic stimulation of cardiac L-type calcium channels in $Ca_v1.2$ phosphorylation site S1928A mutant mice, J. Biol. Chem. 283 (2008) 34738–34744.
[47] M.A. Davare, J.W. Hell, Increased phosphorylation of the neuronal L-type Ca^{2+} channel $Ca_v1.2$ during aging, Proc. Natl. Acad. Sci. U. S. A. 100 (2003) 16018–16023.
[48] K. Tobise, Y. Ishikawa, S.R. Holmer, M.J. Im, J.B. Newell, H. Yoshie, M. Fujita, E.E. Susannie, C.J. Homcy, Changes in type VI adenylyl cyclase isoform expression correlate with a decreased capacity for cAMP generation in the aging ventricle, Circ. Res. 74 (1994) 596–603.
[49] H.J. Yu, H. Ma, R.D. Green, Calcium entry via L-type calcium channels acts as a negative regulator of adenylyl cyclase activity and cyclic AMP levels in cardiac myocytes, Mol. Pharmacol. 44 (1993) 689–693.
[50] T.C. Mou, N. Masada, D.M. Cooper, S.R. Sprang, Structural basis for inhibition of mammalian adenylyl cyclase by calcium, Biochemistry 48 (2009) 3387–3397.
[51] B.L. Prosser, C.W. Ward, W.J. Lederer, Subcellular Ca^{2+} signaling in the heart: the role of ryanodine receptor sensitivity, J. Gen. Physiol. 136 (2010) 135–142.
[52] C. Soeller, M.B. Cannell, Numerical simulation of local calcium movements during L-type calcium channel gating in the cardiac diad, Biophys. J. 73 (1997) 97–111.
[53] D. Willoughby, D.M. Cooper, Organization and Ca^{2+} regulation of adenylyl cyclases in cAMP microdomains, Physiol. Rev. 87 (2007) 965–1010.
[54] T.C. Rich, T.E. Tse, J.G. Rohan, J. Schaack, J.W. Karpen, In vivo assessment of local phosphodiesterase activity using tailored cyclic nucleotide-gated channels as cAMP sensors, J. Gen. Physiol. 118 (2001) 63–78.
[55] A.R. Marks, Ryanodine receptors/calcium release channels in heart failure and sudden cardiac death, J. Mol. Cell. Cardiol. 33 (2001) 615–624.
[56] X.W. Zhou, M. Mudannayake, M. Green, M.S. Gigena, G. Wang, R.F. Shen, T.B. Rogers, Proteomic studies of PP2A-B56gamma1 phosphatase complexes reveal phosphorylation-regulated partners in cardiac local signaling, J. Proteome Res. 6 (2007) 3433–3442.
[57] M.A. Davare, M.C. Horne, J.W. Hell, Protein phosphatase 2A is associated with class C L-type calcium channels ($Ca_v1.2$) and antagonizes channel phosphorylation by cAMP-dependent protein kinase, J. Biol. Chem. 275 (2000) 39710–39717.
[58] J. Satin, E.A. Schroder, S.M. Crump, L-type calcium channel auto-regulation of transcription, Cell Calcium (2011).
[59] J.H. Ahn, T. McAvoy, S.V. Rakhilin, A. Nishi, P. Greengard, A.C. Nairn, Protein kinase A activates protein phosphatase 2A by phosphorylation of the B56delta subunit, Proc. Natl. Acad. Sci. U. S. A. 104 (2007) 2979–2984.
[60] V. De Arcangelis, D. Soto, Y. Xiang, Phosphodiesterase 4 and phosphatase 2A differentially regulate cAMP/protein kinase a signaling for cardiac myocyte contraction under stimulation of beta1 adrenergic receptor, Mol. Pharmacol. 74 (2008) 1453–1462.
[61] S.N. Yang, J. Yu, G.W. Mayr, F. Hofmann, O. Larsson, P.O. Berggren, Inositol hexakisphosphate increases L-type Ca^{2+} channel activity by stimulation of adenylyl cyclase, FASEB J. 15 (2001) 1753–1763.
[62] J. Neumann, Altered phosphatase activity in heart failure, influence on Ca^{2+} movement, Basic Res. Cardiol. 97 (Suppl. 1) (2002) I91–I95.
[63] X. Chen, V. Piacentino 3rd, S. Furukawa, B. Goldman, K.B. Margulies, S.R. Houser, L-type Ca^{2+} channel density and regulation are altered in failing human ventricular myocytes and recover after support with mechanical assist devices, Circ. Res. 91 (2002) 517–524.